water

MDPI

Article

Modeling the Influence of Climate Change on the Water Quality of Doğancı Dam in Bursa, Turkey, Using Artificial Neural Networks

Aslıhan Katip [1,*] and Asifa Anwar [2]

[1] Environmental Engineering Department, Faculty of Engineering, Bursa Uludag University, Görükle Campus, Bursa 16059, Turkey
[2] Division of Sustainable Development, College of Science and Engineering, Hamad Bin Khalifa University, Qatar Foundation, Doha 34110, Qatar; asan39545@hbku.edu.qa
* Correspondence: aballi@uludag.edu.tr

Abstract: Population growth, industrialization, excessive energy consumption, and deforestation have led to climate change and affected water resources like dams intended for public drinking water. Meteorological parameters could be used to understand these effects better to anticipate the water quality of the dam. Artificial neural networks (ANNs) are favored in hydrology due to their accuracy and robustness. This study modeled climatic effects on the water quality of Doğancı dam using a feed-forward neural network with one input, one hidden, and one output layer. Three models were tested using various combinations of meteorological data as input and Doğancı dam's water quality data as output. Model success was determined by the mean squared error and correlation coefficient (R) between the observed and predicted data. Resilient back-propagation and Levenberg–Marquardt were tested for each model to find an appropriate training algorithm. The model with the least error (1.12–1.68) and highest R value (0.93–0.99) used three meteorological inputs (air temperature, global solar radiation, and solar intensity), six water quality parameters of Doğancı dam as output (water temperature, pH, dissolved oxygen, manganese, arsenic, and iron concentrations), and ten hidden nodes. The two training algorithms employed in this study did not differ statistically ($p > 0.05$). However, the Levenberg–Marquardt training approach demonstrated a slight advantage over the resilient back-propagation algorithm by achieving reduced error and higher correlation in most of the models tested in this study. Also, better convergence and faster training with a lesser gradient value were noted for the LM algorithm. It was concluded that ANNs could predict a dam's water quality using meteorological data, making it a useful tool for climatological water quality management and contributing to sustainable water resource planning.

Keywords: artificial neural networks; climate change; Doğancı dam; training algorithms; water quality

Academic Editors: Bahram Gharabaghi, Hossein Bonakdari and Silvio José Gumiere

Received: 12 December 2024
Revised: 21 February 2025
Accepted: 25 February 2025
Published: 2 March 2025

Citation: Katip, A.; Anwar, A. Modeling the Influence of Climate Change on the Water Quality of Doğancı Dam in Bursa, Turkey, Using Artificial Neural Networks. *Water* **2025**, *17*, 728. https://doi.org/10.3390/w17050728

1. Introduction

Water quality has a crucial role in an aquatic system. The quality of the water depicts the extent of water pollution. Likewise, the water quality of surface waters and dams or reservoirs is of paramount importance because humans rely on them to fulfill their daily requirements. In some areas, dam water is rapidly polluted due to the contaminants and sediments from the flooded river water. Additionally, climate change could cause eutrophication, resulting in algal blooms [1].

An increase in the air temperature due to global warming is also altering the temperature of water bodies, which is one of the main parameters that affect the growth and development of aquatic organisms and the chemical processes occurring within the water bodies [2]. The heating and cooling process of water bodies is highly affected by meteorological parameters, i.e., solar radiation, air temperature, and wind speed [3]. Under these circumstances, predicting water quality would become crucial for ecosystem sustainability, environmental monitoring, and human sustenance.

Artificial neural network modeling could provide a meaningful understanding of water quality and meteorological parameters [4]. Based on the supplied data, ANNs can make predictions about the changing trend of water quality at a specific point in the future [5]. Due to the complexity, traditional methods such as linear, dynamic, or stochastic programming are not preferable for predictions, as these are not efficient enough to handle extensive data [6]. Some previously established water quality prediction models, such as multiple linear regression (MLP) or auto-regressive integrated moving average (ARIMA) models, have been studied [7,8]. However, MLP is limited in capturing non-linear relationships because of its inherently linear structure [9], while ARIMA also has the drawback of not being able to analyze non-linear time series for predictions. Such conventional methods have been reported to be incompetent in dealing with multipurpose reservoirs [10]. Earlier studies claimed that evolutionary techniques were far more capable than classical techniques and could successfully handle large data with various objective functions [11]. In addition, unlike conventional statistical methods, ANNs require fewer prior assumptions and attain greater precision [12]. Multiple studies conducted on water quality indicated the superiority of ANNs' predictive performance over regression models [7,13,14].

Researchers have used ANNs to predict water quality in dams. ANNs were chosen for the Monte Novo dam in Portugal to estimate oxidizability, measuring pH, conductivity, dissolved oxygen (DO), water temperature, and stored water volume [15]. ANNs were also used to estimate DO concentration in Feitsui reservoir in Northern Taiwan [16]. In 2017, an ANN predicted the total dissolved solids (TDS) in the Karaj dam [17]. One study determined water quality in Taiwan reservoirs using ANNs, support vector machines, classification and regression trees, and linear regression. Data from 1995–2016 (1635 values) were collected for surface water temperature, biological oxygen demand (BOD), total suspended solids (TSS), chemical oxygen demand (COD), and ammonia (NH_3) concentration and pre-processed as inputs to the modeling system. The pre-processing was completed by removing the rows with incomplete data for accurate modeling. The comparison showed that the ANN model was more accurate than conventional hydrological statistical methods [18].

ANNs are also considered when studying the effects of climate change on water quality. After applying previous hydrological climate change scenarios to the Namgang dam basin precipitation–runoff model, water quality (suspended solids, total nitrogen, total phosphorus, dissolved oxygen, biological oxygen demand, and chlorophyll-a) under climate change was estimated [19]. In 2015, an ANN estimated eutrophication for the Yuqiao reservoir in North China, the city's potable water source. The reservoir was found to be threatened by eutrophication due to the changing climate [20]. Eutrophication and temperature at Dez dam in Iran in 2015 were evaluated using feed-forward ANNs [21]. In 2017, a study applied the ANN tool to Adelaide, South Australia's drinking-water semi-arid Millbrook catchment-reservoir system. Modeling took into account precipitation, maximum and minimum temperature, solar radiation, relative humidity, and wind speed [22]. Considering meteorological factors, an advanced dynamic regression neural network predicted total nitrogen and phosphorus in the Shi River reservoir for 2021 [23].

ANNs have been employed to study Turkey's changing water quality in certain dams and water bodies. Eutrophication in Köyceğiz lake was evaluated using the ANN approach [24]. The chlorophyll-a concentration in Keban dam was also estimated using alkalinity, pH, water temperature, electrical conductivity, and dissolved oxygen, phosphate, and nitrate concentrations as inputs to neural networks [25].

In terms of climate change, the effect of meteorological factors (precipitation, evaporation, relative humidity, temperature, and wind speed) on the water quality of Sapanca lake in long-term water supply was determined [26]. For the Mamasin dam, rainfall measurements with the dam's temperature, total suspended solids, and total nitrogen concentrations were used to find the electrical conductivity and dissolved oxygen using the ANN model with feed-forward and back-propagation architecture [27]. The change in meteorological data over a long period of time is directly linked to climate change, i.e., the rise in the air temperature over the past few years is a sign of global warming, or the shift in global precipitation patterns gives an indication of an imbalance in hydrological cycles [28–30]. As a result, it also alters the water quality of dams, rivers, lakes, etc. [31]. Therefore, meteorological parameters are effectively used in hydrological modeling to capture climatic impacts.

As predicted by the Intergovernmental Panel on Climate Change (IPCC) Representative Concentration Pathway (RCP) 8.5 scenario, the temperature will increase by 2 °C in the summer months between 2020 and 2050, compared to 1970 to 2000 in the Mediterranean climate zone, including Turkey [32]. Therefore, forecasting the quality of drinking-water resources, one being dams, is essential for livelihood.

Doğancı dam is one of the primary water resources, along with the Nilufer dam, for the population residing in Bursa, Turkey. Bursa's drinking-water resources had decreased due to a population increase of 2.3% and unplanned urbanization [33]. Also, it was observed that Doğancı dam's water quality had declined, especially with the increased heavy metal concentration [34]. In the 21st century, the temperature in Bursa also increased by 0.5 °C compared to the last century. A study was conducted using the standardized precipitation index (SYI) for Bursa in 2019, and it forecasted a drought that would continue for a while [35]. ANNs also modeled the meteorological drought in Bursa in a study named "Meteorological Drought Analysis Using ANN for Bursa Province" [36], which predicted the chances of drought in the city.

Because the scenarios regarding climate change are based on changes in meteorological parameters over a 30-year period [29], the current research focused on evaluating the impact of climate change on the water quality of Doğancı dam, utilizing artificial neural networks and modeling with a unique combination of meteorological parameters. Notably, this study is novel in the local context for using artificial neural networks to assess how different climate indicators affect the dam's water quality. The analysis included specific meteorological parameters like snow depth and evapotranspiration, which had not been used in similar research, adding a distinct and innovative perspective for understanding climate impacts on water quality.

As climate change continues to impact water resources throughout the globe, understanding its impact on water quality is critical for ensuring the sustainability of drinking-water supplies. This research addressed the broader international concern of water scarcity and quality degradation due to increasing temperatures, shifting precipitation patterns, and other climatic effects, which threaten water security globally.

2. Materials and Methods

2.1. Study Area

Doğancı dam (Figure 1), situated in Bursa, Turkey, serves as an essential water supply for the city's population [37]. Bursa, Turkey's fourth most populous city, is uniquely positioned between the Marmara and Aegean regions, resulting in a climate that varies from Mediterranean in the northern parts to continental in the southern and inner areas. Bursa is divided into different districts: Osmangazi, Yildrim, Nilufer, Gursu, and Kestel [38]. The dam itself, crucial for the city's water needs, boasts a body fill volume of 2,520,000 m^3 and a height of 65 m from the riverbed and provides about 125 hm^3 of potable water annually [39]. This study focused on the dam within the context of Bursa's diverse climatic conditions, emphasizing the importance of assessing climate change impacts on such a vital water resource.

Figure 1. Satellite view of Doğancı dam (acquired from Google Maps on 10 January 2024).

2.2. Modeling Data

In this study, the acquisition of valid data was of significant importance. Bursa has 16 meteorological stations distributed in different districts across the city. Monthly data from these 16 stations were collected from the Meteorological Department in Bursa, working under the Ministry of Forestry and Water Affairs. Likewise, monthly water quality data for Doğancı dam were obtained from Bursa's Water and Sewage Authority. The meteorological and water quality data obtained were noted from 1990 to 2019 and consisted of monthly average values for each parameter. The use of monthly data is common in water quality modeling, incorporating meteorological data, and using ANNs [9,40–42], as it reduces the short-time noise and enables faster training of the models while capturing long-term trends.

The original data were initially available in scattered hard copies and had a few occasional missing records. Hence, the data points for all the parameters were transferred to an Excel (Version 2501) worksheet. Data imputation and removal were performed based on its trend to ensure data consistency. A minor number of values in the dataset appeared to be unrealistic (possibly due to manual reporting), so these outliers were removed. Likewise, the missing values, which were very minimal, were filled using near data points and applying interpolation. This approach preserved the local trend of the dataset and the overall integrity of the data used for modeling. Linear interpolation has been evaluated as a suitable method for treating time-series data [43].

Meteorological data consisted of monthly average values of certain parameters, i.e., vapor pressure (hPa), relative humidity (%), air temperature (°C), wind speed (m/s), precipitation (mm), global solar radiation (kWh/m^2), solar intensity (cal/cm^2), evapotranspiration (mm), snow depth (cm), and evaporation (mm). The long-term meteorological data considered over 30 years [22] serve as an indicator of climate change. These meteorological parameters have been reported in the literature as inputs to model the climatic effects on the water quality of a water body. The meteorological parameters that best indicate climate change are air temperature, solar radiation and intensity, wind, and pressure, which are indicators of the forces that create air movements. Apart from these, the meteorological parameters that can most clearly show the hydrological cycle are total precipitation, snow depth, relative humidity, and total evaporation [22,44]. For the water quality of Doğancı dam, the parameters included monthly average values of pH, turbidity (NTU), water temperature (°C), TSS (mg/L), DO (mg/L), alkalinity (mg/L), and concentrations of certain trace elements such as iron (µg/L), manganese (µg/L), and arsenic (µg/L). The statistical values for the acquired data are listed in Tables 1 and 2.

Table 1. Statistics of Bursa's meteorological data from 1990 to 2019.

Parameters	Range for the Overall Data (Mean ± Standard Deviation)
Monthly average vapor pressure (hPa)	4.65–22.52 (11.92 ± 4.53)
Monthly average relative humidity (%)	49.11–87.86 (69.19 ± 7.53)
Monthly average air temperature (°C)	1.00–27.64 (14.89 ± 7.22)
Monthly average wind speed (m/s)	0.77–3.30 (1.99 ± 0.46)
Monthly average of total precipitation (mm)	0.00–26.70 (1.94 ± 1.99)
Monthly average of total daily global solar radiation (kWh/m^2)	0.05–7.16 (3.38 ± 2.09)
Monthly average of total daily solar intensity (cal/cm^2)	53.13–644.72 (322.47 ± 155.49)
Monthly average of total evapotranspiration (mm)	0.09–30.15 (4.74 ± 3.38)
Monthly average of total snow depth (cm)	0.00–30.75 (0.97 ± 3.02)
Monthly average of total evaporation (mm)	1.00–13.30 (5.12 ± 2.50)

Table 2. Statistics of monthly average values from 1990 to 2019 for water quality parameters of Doğancı dam.

Parameters (Monthly Monitored Data)	Range for the Overall Data (Mean ± Standard Deviation)	USEPA Standards [a] [45]	WHO Standards [b] [46]	Turkish Standards [47]
pH	7.44–8.45 (8.05 ± 0.23)	6.50–8.50	6.50–8.00	6.50–9.50
Turbidity (NTU)	0.73–85.75 (6.38 ± 7.38)	1.00	5.00	1.00
Water temperature (°C)	5.21–23.21 (12.71 ± 4.29)	-	-	-
Total suspended solids (mg/L)	0.00–38.38 (4.98 ± 5.88)	-	-	-
Dissolved oxygen (mg/L)	0.80–9.91 (5.04 ± 2.83)	-	-	-
Alkalinity (mg/L)	134.00–209.25 (169.12 ± 20.46)	-	-	-
Iron (µg/L)	10.00–175.00 (47.00 ± 32.00)	300.00	300.00	200.00
Manganese (µg/L)	13.00–288.00 (48.00 ± 38.00)	50.00	100.00	50.00
Arsenic (µg/L)	4.00–6.00 (5.00 ± 1.00)	10.00	10.00	10.00

Note(s): [a,b] USEPA stands for the United States Environmental Protection Agency, and WHO is the abbreviation for the World Health Organization.

2.3. Artificial Neural Networks (ANNs)

After accessing the data, the next stage involved modeling using ANNs. The software used was MATLAB (Version R2022a). Similar in principle to the biological nervous system of humans, ANNs are a collection of detailed integrated processing elements that handle a parallel and distributed information system [48]. The operation of the ANN method includes the processing of information or inputs in specific components known as neurons or nodes and the transmission of signals between neurons via communicating links (these links have a particular weight represented as connection density), and, usually, the use of activation functions by each neuron of the ANN architecture specifies the outputs for input variables [49]. An ANN is well suited to fit the best relationships among parameters and monitor all possible relationships based on previous information [50].

In this study, a feed-forward neural network was chosen for modeling the effects of meteorological data on the water quality of Doğancı dam. Types of ANN employed in engineering applications include feed-forward neural networks, convolutional neural networks, and recurrent neural networks. The feed-forward neural network has an output layer and one or more hidden layers. The convolutional neural network has layers that process the inputs to feature maps. It is utilized in image processing. Lastly, the recurrent neural networks model deals with inputs in time series using feedback loops [51,52]. A feed-forward neural network was chosen based on its successful application in relevant studies [15,17,18,24,25,53]. A general architecture of a multi-layer feed-forward neural network is given in Figure 2.

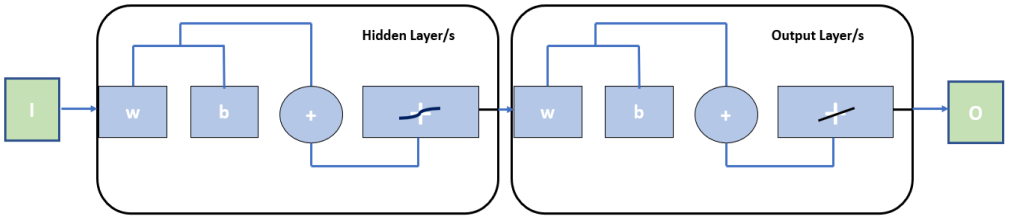

Figure 2. Feed-forward neural network (acquired from MATLAB).

In Figure 2, I represents the input; w and b are for the weight of neurons and bias values, respectively; and O is for the output. The output of the neural network could be equated to the following:

$$\text{Output} = f(a) \quad (1)$$

where f denotes the activation function, and a is the neuron signal that is defined as

$$a = \sum_{i=1}^{Z} w_i x_i + bi \quad (2)$$

where w_i is the weight of the input neuron x_i. Z represents the total number of inputs. The summation stages occur at each hidden neuron i. Typically, the sum of every input neuron is weighed and then processed through an activation function, which is a non-linear function [54,55].

2.4. Training Algorithms

The present study used two training algorithms, i.e., resilient back-propagation and Levenberg–Marquardt algorithms, to determine which algorithms train the model best and present accurate models while using feed-forward neural networks. The main aim of the training was to reduce the mean squared error (MSE) and obtain a higher value for

regression coefficient R. A higher R value means a good correlation between observed and predicted values. MSE is generally calculated as follows:

$$MSE = \frac{1}{N}\sum_{j=1}^{N}(y_j - \hat{y}_j)^2 \quad (3)$$

N is the total number of output values, y_j denotes the observed output value, and $\hat{y}_j$ is the predicted output value. The lower the value of error, the better the prediction would be when comparing the training algorithms. The values would represent the minimum difference between the actual and modeled output values [56].

2.4.1. Levenberg–Marquardt Algorithm

The Levenberg–Marquardt (LM) algorithm approximates the Hessian matrix as follows:

$$c_{k+1} = c_k - \left(J^T J + \mu I\right)^{-1} J^T e \quad (4)$$

where c_k is the gradient of the algorithm, J represents the Jacobian matrix (containing first derivates of errors in line with weights and biases of the neurons), and e denotes the vector of network errors. μ is a scalar quantity of the algorithm. μ is decreased after each run by a reduction in the performance function in each algorithm iteration. Momentum update (Mu) is a control or adaptation parameter of the LM algorithm for updating the weights while training the neural networks and allowing proper convergence. The range of Mu is between 0 and 1. The LM training algorithm is better at optimization when using feed-forward networks than other conventional gradient-descent techniques [57].

2.4.2. Resilient Back-Propagation Algorithm

Sigmoid transfer functions are frequently used in hidden layers in multi-layer feed-forward neural networks. The slope of sigmoid functions decreases as the input size increases until it reaches zero. Because the gradient might have a very small magnitude even when the weights and biases are far from their ideal values, this could result in little changes to the weights and biases. The resilient back-propagation (RProp) training method seeks to eliminate the variable effects of the partial derivative magnitudes. A different updated value determines the extent of the weight shift. When the derivative of the performance function for a weight has the same sign for two iterations, each weight and bias is increased by a factor. The updated value is lowered by a factor whenever the weight derivative changes sign. Zero derivatives keep the updated value the same [57].

3. ANN Application in the Current Study

As mentioned, a feed-forward neural network was employed, having one input layer, an intermediate hidden layer, and an output layer. In this study, 70% of the provided data were used for training the models (i.e., 252 values for each parameter), and the remaining 30% was used for testing and validation [19,20]. Before training the models, data normalization was performed using the following equation:

$$D = \frac{D_i - D_{min}}{D_{max} - D_{min}} \quad (5)$$

where D represents a dimensionless normalized value. In contrast, D_i is the normalized value for the ith measurement in the data, and D_{max} and D_{min} are the maximum and minimum normalized scores, respectively, of all the training and testing data taken.

The software normally adjusts weights and bias values based on the error value during training. If the network overfits the data, the MSE value increases during validation. On

the other hand, the testing data verified the performance of the model. Here, the feed-forward neural network used a sigmoid activation function in the hidden layer and a linear activation function in the output layer, which was recommended for a robust result [58]. The target epochs were set to 1000 [59]. The number of nodes in the hidden layer was selected on a hit-and-trial basis, which is a common technique used by most researchers in ANN modeling [60–63]. Hidden nodes varying from one to fifty were tested. The observations indicated that as the number of nodes increased from one to ten, there was a noticeable improvement in performance of the models in terms of higher R^2 values and lower MSEs. However, beyond ten nodes, the models' performance began to decrease, which can be attributed to overfitting. So, ten hidden nodes were selected for each model.

In this study, meteorological parameters were taken as inputs, and the water quality parameters of the dam were defined as the outputs of the neural architecture. In order to better understand the effects of climate change, the meteorological parameters had been grouped from three different perspectives. Inputs and outputs created according to three groupings were modeled and tested. Temperature and pH were selected as common parameters in the three-model structure to create the outputs. The first model aimed to model trace elements, the second model to model trace elements together with suspended solids and turbidity, and the third model to model only suspended solids and turbidity. In the first model, to examine the variations in the effects of temperature and solar radiation in climate change, air temperature, global solar radiation, and solar intensity were taken as input parameters. In the second defined model, in order to examine the effect of air movements in climate change, wind speed, evaporation, vapor pressure, and evapotranspiration were the input parameters. Lastly, precipitation, snow depth, and humidity parameters, which partly show the effects of the hydrological cycle in climate change, were grouped as inputs. The modeling aimed to identify which model gave the best predictions regarding output parameters, i.e., Doğancı dam's water quality. These groupings in the inputs were made to show which meteorological events in the atmosphere have the greatest impact on climate change and water quality.

4. Results and Discussion

It can be noted from Table 1 that the minimum monthly average air temperature from 1990 to 2019 was 1 °C. On the other hand, the minimum monthly average temperature of the water over the considered study years was 5.21 °C (Table 2). Nevertheless, the maximum monthly average temperature of the water was less than that of the air. This could be because the water's unique high heat capacity, i.e., hydrogen bonds, strongly holds water molecules together. It can absorb high amounts of heat without increasing the temperature. The second noticeable feature was the concentration of a few trace elements in Doğancı dam's water. The highest monthly average concentration from 1990 to 2019 was manganese (48 µg/L), while the lowest was arsenic (5 µg/L). The mean of the monthly average values for manganese seemed to be just touching the limit prescribed by the USEPA and TS 266 drinking-water quality standards, with the maximum monthly average value (288 µg/L) exceeding all the considered drinking-water quality standards. This issue could be alarming, as higher concentrations of manganese in drinking-water consumption could lead to neurological diseases in humans [46]. The mean values for the monthly average concentrations of iron and arsenic seemed to be well within the limits for drinking-water standards. However, even in the case of arsenic, small concentrations could be threatening with long-term exposure per USEPA guidelines [64]. Looking at the turbidity values, the average value for Doğancı dam was 6.378 NTU, which was higher than the limits for drinking water defined by WHO, USEPA, and Turkish standards. The increase in turbidity could be due to erosion resulting from stronger storms, higher water levels, or increased

water velocity in the dam due to climate change. Nevertheless, this could potentially have an adverse effect on the humans relying on the water from Doğancı dam.

The results obtained from modeling using multi-layer feed-forward neural networks are given in Table 3. Considering Model 1, for the three meteorological inputs (air temperature, global solar radiation, and solar intensity) and six corresponding outputs of Doğancı dam's water quality (water temperature, pH, dissolved oxygen, manganese, arsenic, and iron concentrations), we concluded that the run was quite successful. The R values for the training, testing, validation, and whole dataset were between 0.93 and 0.99, showing a strong correlation between the observed and the predicted data. The mean squared error (MSE) achieved in this study was notably low, with an approximate value of 1.20 when using the LM algorithm and 1.68 with the RProp algorithm.

Table 3. Results obtained from modeling using the feed-forward neural networks.

Model	Input	Output	ANN Structure	Performance Checks				
				R-Value				MSE
				Training	Testing	Validation	Whole Dataset	
1	Monthly average: • air temperature (°C) • total daily global solar radiation (kWh/m^2) • total daily solar intensity (cal/cm^2)	Monthly average: • water temperature (°C) • pH • concentration of dissolved oxygen (mg/L) • concentration of arsenic (µg/L) • concentration of manganese (µg/L) • concentration of iron (µg/L)	3-10-6	RProp: 0.99031 LM: 0.99252	RProp: 0.93702 LM: 0.93271	RProp: 0.97481 LM: 0.98139	RProp: 0.98246 LM: 0.98419	RProp: 1.6807 LM: 1.1995
2	Monthly average: • wind speed (m/s) • total evaporation (mm) • vapor pressure (hPa) • total evapotranspiration (mm)	Monthly average: • water temperature (°C) • pH • turbidity (NTU) • concentration of dissolved oxygen (mg/L) • concentration of suspended solids (mg/L) • concentration of arsenic (µg/L) • concentration of iron (µg/L)	4-10-7	RProp: 0.81675 LM: 0.89479	RProp: 0.85025 LM: 0.73438	RProp: 0.74738 LM: 0.84478	RProp: 0.80832 LM: 0.85980	RProp: 11.9053 LM: 6.2589
3	Monthly average: • total precipitation (mm) • snow depth (cm) • relative humidity (%)	Monthly average: • water temperature (°C) • pH • alkalinity (mg/L) • turbidity (NTU) • concentration of suspended solids (mg/L) • concentration of dissolved oxygen (mg/L) • concentration of arsenic (µg/L) • concentration of manganese (µg/L) • concentration of iron (µg/L)	3-10-9	RProp: 0.69934 LM: 0.68462	RProp: 0.51694 LM: 0.35175	RProp: 0.74147 LM: 0.74684	RProp: 0.66439 LM: 0.57835	RProp: 11.011 LM: 11.1604

In Model 2, the R value, indicating the correlation between observed and predicted data, ranged from 0.81 to 0.86 using both training algorithms. This model showed a good but slightly weaker correlation compared to Model 1. Additionally, the MSE was higher in Model 2, with values ranging from 6.26 to 11.91 for the algorithms tested.

In the final model, nine water quality parameters were analyzed, including water temperature, pH, alkalinity, turbidity, dissolved oxygen, suspended solids, arsenic, manganese, and iron, with precipitation, snow depth, and relative humidity as inputs. This model exhibited a lower correlation coefficient for the entire dataset, ranging from 0.58 to

0.66, suggesting a weaker predictive accuracy compared to the first two models. The MSE values were higher in this model, recorded at 11.01 using the RProp algorithm and 11.16 with the LM algorithm, surpassing the values observed in Model 1.

Comparing all the tested models, we observed that Model 1 showed a greater reliability in prediction with a lower MSE (1.20–1.68) and a higher R (0.93–0.99) between the observed and predicted values for all stages of neural networking. It must be noted that the algorithms used in the modeling were the same; the results differed because of the choice of input parameters. ANNs modify the internal weights and biases according to the input data, which results in varying output results [65–67].

The better correlation in Model 1 could also be explained by the direct impact of the input parameters on the output parameters. The air temperature, global solar radiation, and solar intensity directly influence water quality parameters such as temperature, pH, and dissolved oxygen. Research by Soro, et al. [68] showed that an increase in the air temperature leads to an increase in the water temperature and, simultaneously, a decrease in the dissolved oxygen levels of a freshwater body. Also, temperature and solar radiation were the most important parameters in modeling climate change [29]. Therefore, the selection of model input variables enhanced the predictive capability of ANNs in water quality modeling [65]. Additionally, Model 1's architecture was the simplest; it involved only three input parameters and, correspondingly, six output parameters, which could have reduced complexity, offered better generalization, and reduced prediction errors. A complex architecture in ANNs is shown to display high training time and higher prediction errors [69]. Therefore, relevant input parameters, maintaining model simplicity, and utilizing an efficient training algorithm could significantly enhance the performance of ANN models.

This argument is further strengthened by looking at Figure 3, which compares the R values obtained for the whole datasets of all the models. The term 'data' in Figure 3 represents the actual target values from the dataset, while 'fit' gives the predictions generated by the ANN. The dotted line (Y = T) is the line of perfect fit, where the predictions exactly match the actual values.

It was seen that the data points are homoscedastic (with very few outliers) in Model 1, which demonstrates its reliability in prediction. The close spread of the data points across the line of perfect fit (Y = T) and the solid 'fit' line sitting exactly on the dotted line demonstrate consistency between the observed and predicted values. However, the solid line can be seen to deviate from the dotted lines in Model 2 and Model 3, suggesting less accuracy due to a difference between the predicted and actual data.

Mean squared error graphs are depicted in Figure 4. The graphs for the mean squared errors provided critical insights into the models regarding their training dynamics and generalization capabilities. Model 1 displayed a rapid decline in MSE values for the training dataset in the early epochs (particularly while using the LM training algorithm), indicating efficient learning. However, as the training progressed, a divergence was seen between the training error and the test/validation errors, indicating overfitting. Despite that, the validation and test errors stabilized at relatively lower values, which showed that Model 1 achieved accurate predictions across datasets and prioritized high accuracy.

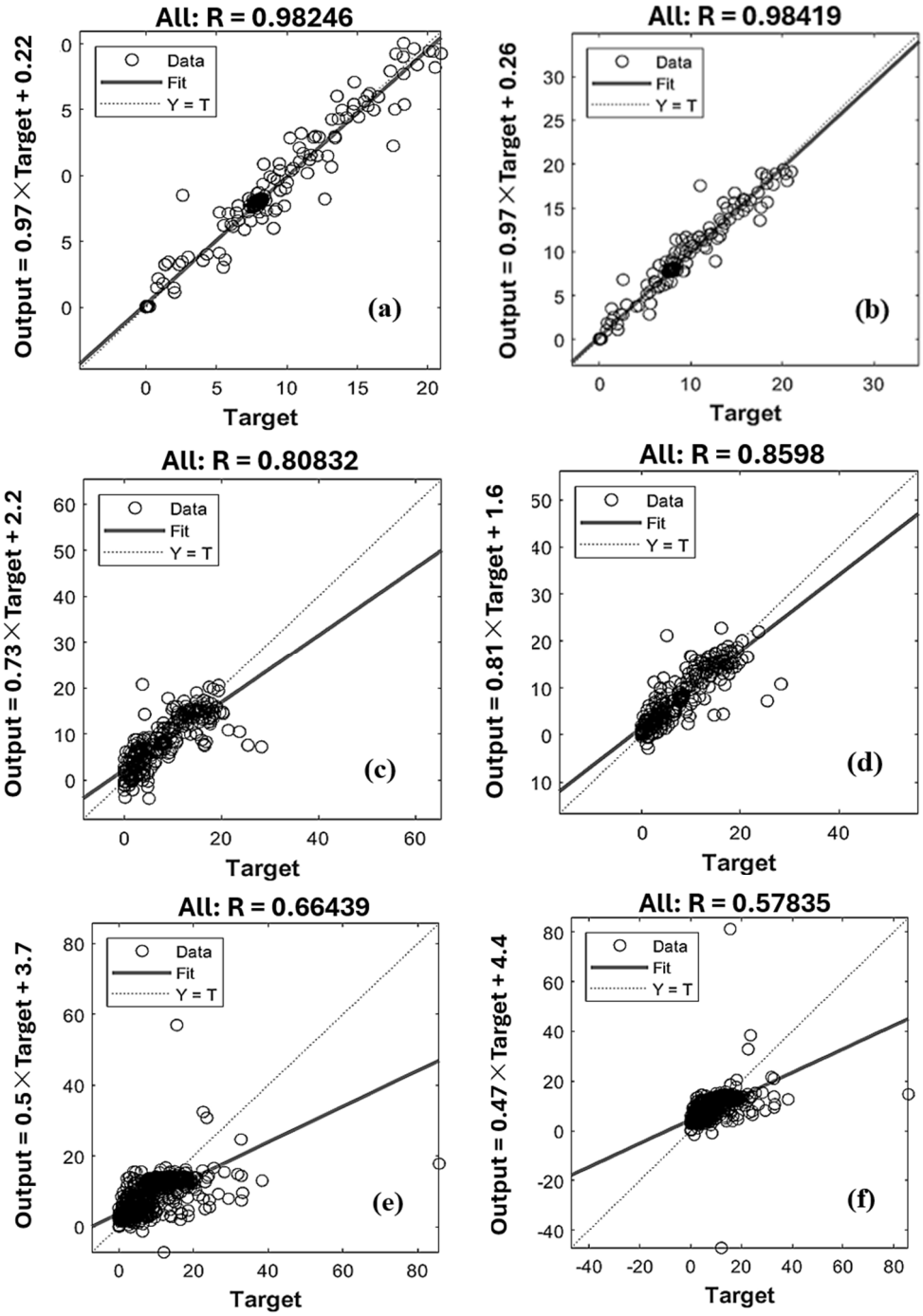

Figure 3. Graphs of the correlation coefficients of models using the RProp ((**a**) Model 1, (**c**) Model 2, and (**e**) Model 3) and the LM ((**b**) Model 1, (**d**) Model 2, and (**f**) Model 3) training algorithms.

In contrast to Model 1, Model 2 exhibited lower divergence. The training, validation, and test errors decreased steadily. Nevertheless, the overall MSE values were higher than those of Model 1, which suggested that Model 2 may not capture the complexity of the datasets, resulting in slightly less accurate predictions. Model 3 performed the poorest of the three models. The MSE values for Model 3 using the LM and RProp algorithms remained higher across all the datasets, and there was a divergence between the training, validation, and test errors noted. Therefore, Model 3 had limited predictive accuracy and weak generalization capabilities.

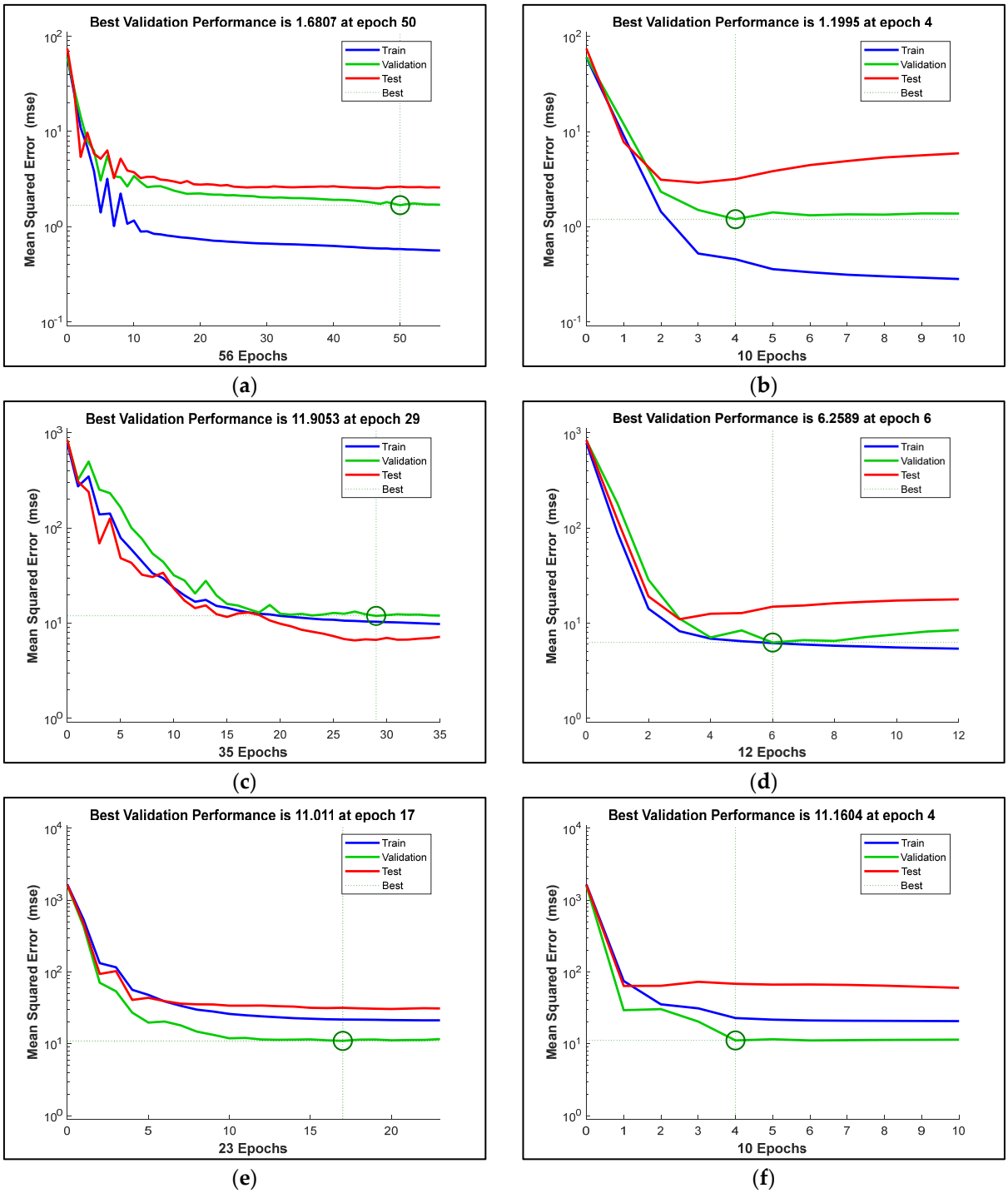

Figure 4. Mean squared errors of the models using the RProp ((**a**) Model 1, (**c**) Model 2, and (**e**) Model 3) and the LM ((**b**) Model 1, (**d**) Model 2, and (**f**) Model 3) training algorithms.

Additionally, higher fluctuations could be seen in the MSE graphs of Model 2 as compared to Model 1. The fluctuations indicated that the model is less stable and less reliable for effective predictions. Thus, Model 1 emerged as the best model, as previously described.

The results can be further validated by comparing the parameters of the training progress for the models, as listed in Table 4. The parameters examined included the gradient at the point of ending of the training. The stop epoch represented the number of epochs required for training to conclude.

Table 4. Training state parameters for the models using the defined algorithms.

Models	Training Algorithms	Training Progress Parameters		
		Gradient	Mu	Stop Epoch
Model 1	Levenberg–Marquardt	0.143	0.001	10
	Back-propagation	0.397	-	56
Model 2	Levenberg–Marquardt	4.26	0.01	12
	Back-propagation	6.4	-	35
Model 3	Levenberg–Marquardt	4.47	0.1	10
	Back-propagation	20.1	-	23

Model 1, trained with Levenberg–Marquardt, exhibited the most efficient training, achieving a minimum gradient value of 0.143 and completing the training in just 10 epochs. This performance was better than when it was trained with back-propagation. In terms of the other tested models, Model 3 demonstrated the least effective convergence, particularly when trained with a back-propagation algorithm. Models 2 and 3 had higher gradients than Model 1 at the termination point.

The results from the training progress also demonstrated that Levenberg–Marquardt consistently required fewer epochs to reach convergence, as seen by the stop epoch values ranging from 10 to 12 across all the models. Hence, LM was found to be computationally more efficient compared to back-propagation, which required significantly more training epochs (23 to 56 epochs). The gradient values from the LM algorithm were also generally smaller, with Model 1 achieving the smallest gradient of 0.143, suggesting closer proximity to an optimal solution. The gradient was notably higher in the case of back-propagation, particularly for Model 3, where it reached 20.1. The findings suggested that Model 1 performed better in terms of training when using the Levenberg–Marquardt algorithm.

Mu is specific to the Levenberg–Marquardt algorithm, which reflects the adjustment factor during optimization. Model 1 shows the lowest Mu value of 0.001, followed by Model 2 at 0.01 and Model 3 at 0.1. As seen in Model 1, a smaller Mu value corresponded to faster convergence and better optimization stability. This conclusion also aligned with the observation that Model 1 had the smallest gradient and needed the fewest epochs among the other models to complete the training step.

The graphs for the gradients during the training of the models are given in Figure 5. The gradient of Model 1 settled at a smaller value of 0.143–0.397. Based on the trends, Model 1 stood out as the most optimized configuration due to its rapid and reasonably stable gradient reduction and minimum gradient value, followed by Models 2 and 3 under the LM algorithm. RProp demonstrated slower and inconsistent performance in gradient graphs across all the models when comparing the training algorithms.

It has also been documented in the literature that the resilient back-propagation algorithm has several limitations, including slow training time, the need for extensive training, temporal instability that may cause oscillations during the learning process, and a tendency to become trapped in local minima. In contrast, the LM algorithm undergoes faster convergence, making it more efficient and reliable for training ANNs [70,71].

A comparison was made between the current study's performance checks (R and MSE) with those of similar studies from the literature (Table 5). The correlation coefficient range for a similar study by Kang, et al. [19] was between 0.66 and 0.71 for testing and validation. Likewise, in the study by Park, et al. [72], the value for correlation lay between 0.71 and 0.74. The correlation coefficient acquired in this study for Model 1 (0.93 to 0.99) was higher than that in previously mentioned studies. Also, comparing the attained R values with those of the analysis by Zhang, et al. [20] for all the stages of neural networking,

i.e., training, testing, and validation, we observed that the values for the proposed Model 1 remained higher.

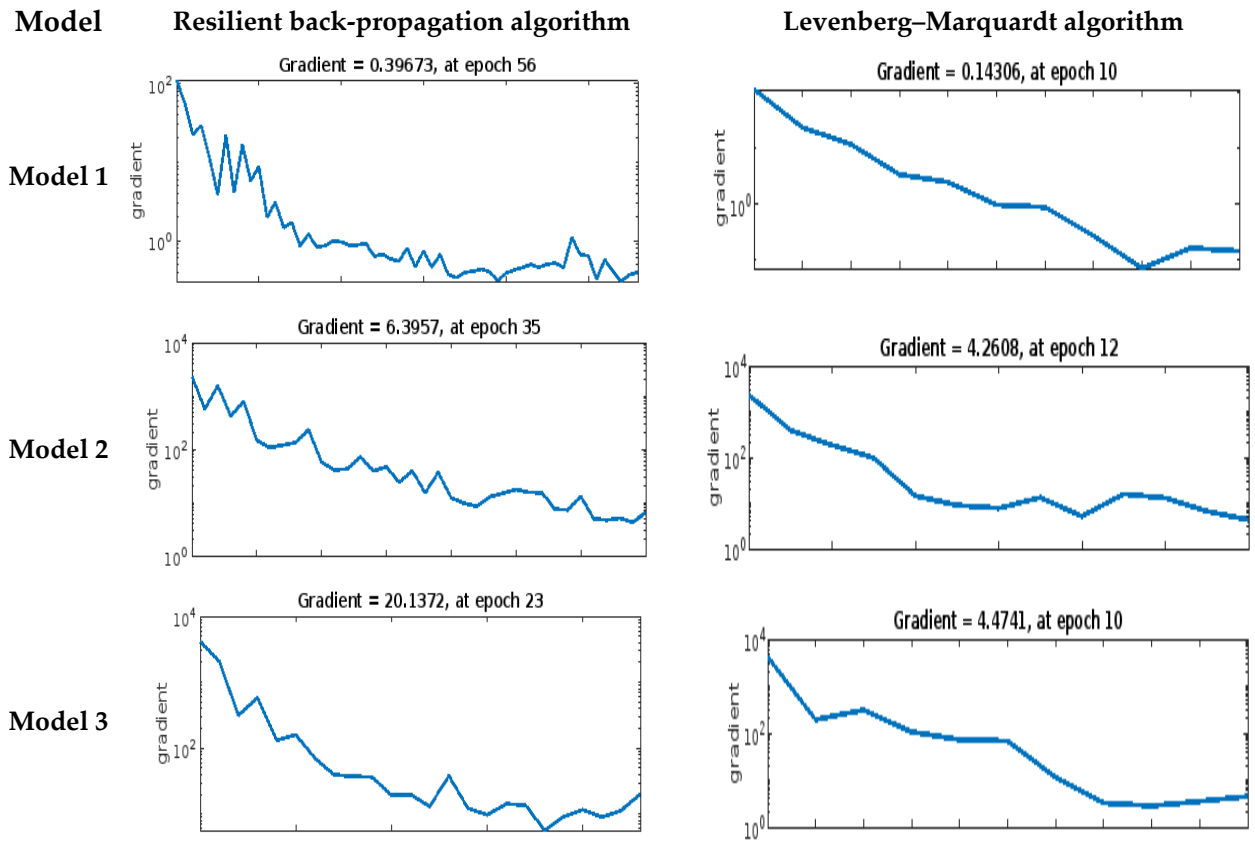

Figure 5. Gradients during training progress using different algorithms for the tested models.

Table 5. References for previous studies predicting the water quality of dams using meteorological parameters.

Study No.	Input (Meteorological Parameter/s)	Output (Water Quality Parameter/s for the Dam)	Structure of Feed-Forward Neural NetWork	Correlation Coefficient [c]	Error [d]	Reference
1.	Precipitation, temperature, and humidity	Suspended solids, total nitrogen, and total phosphorus	1 input, 1 hidden, and 1 output layer	0.66–0.71	0.11–3.12	[19]
2.	Temperature, precipitation, and sunshine hours	Water temperature, total phosphorus, and chlorophyll-a	1 input, 3 hidden, and 1 output layer	0.59–0.99	0.003–0.01	[20]
3.	Solar radiation and wind speed	Chlorophyll-a	1 input, 1 hidden, and 1 output layer	0.71–0.74	-	[72]
4.	Precipitation	Conductivity and dissolved oxygen	1 input, 2 hidden, and 1 output layer	-	0.05–0.06	[27]

Note(s): [c,d] The range for error and correlation coefficient values is for training, testing, and validation.

Another factor considered was the error values, which, in previously reported studies, were as low as 0.003 and reached 3.12 (Table 5). The error values for Studies 2 and 4 listed in Table 5 were lower than those for the proposed Model 1. However, they were within the range of those found for Study 1, with the upper limit (3.12) being higher than that of the proposed model (i.e., 1.20–1.68).

Therefore, it could be concluded that the model proposed is sufficiently valid for future predictions of the water quality of Doğancı dam. It was also noted that the R and

MSE values relied on the inputs and outputs taken. The inputs taken for the proposed Model 1 differ from those in the past studies mentioned. The effects that precipitation, air temperature, atmospheric pressure, humidity, wind speed, and solar radiation may have on water quality were typically evaluated. However, in the mentioned best Model 1 of this study, the monthly average air temperature, monthly average total daily global solar radiation, and solar intensity were considered as inputs to analyze their impacts on Doğancı dam's monthly average water temperature, pH, and monthly average concentrations of dissolved oxygen, arsenic, manganese, and iron. It gave reliable results compared to the other models tested in this study and the previous studies discussed.

Moving to the analysis of the resilient back-propagation and Levenberg–Marquardt training algorithms, statistical evaluation (analysis of variance; ANOVA) showed no significant difference between the two training algorithms. This is justified by the p values in Table 6, which were greater than 0.05 at a 95% confidence level (p = 0.946 for R and p = 0.209 for MSE). Also, the effect sizes were very small (0.001 to 0.05), further emphasizing that the difference between the algorithms was negligible. This statistical examination was conducted on JASP (Version 0.16.3) [73].

Table 6. Comparing (a) R values and (b) MSE of the models for training algorithms using ANOVA.

(a)						
Cases	**Sum of Squares**	**df**	**Mean Squared**	**F**	***p***	**η^2**
Algorithms	$1.796e^{-4}$	1	$1.796e^{-4}$	0.005	0.946	0.001
Residuals	0.137	4	0.034			
(b)						
Cases	**Sum of Squares**	**df**	**Mean Squared**	**F**	***p***	**η^2**
Algorithms	5.956	1	5.956	0.209	0.671	0.050
Residuals	113.746	4	28.437			

However, through visual analysis, it could be said that the Levenberg–Marquardt training algorithm had the edge over the resilient back-propagation algorithm based on the correlation and mean squared error values. Looking at the best model, i.e., Model 1, we can see that the correlation coefficient for the whole dataset was 0.984, and the MSE was 1.20 using the Levenberg–Marquardt algorithm. The values were 0.982 and 1.68, respectively, using resilient back-propagation. Although these values were sufficiently near one another, the LM algorithm improved performance comparatively.

Additionally, for the models, when trained with a resilient back-propagation algorithm, the gradient reduction exhibited a generally decreasing pattern (Figure 5), but the process was uneven and slower. There were fluctuations throughout the training process, indicating less stability in the optimization process when using the RProp algorithm. In contrast, the LM algorithm demonstrated a more consistent and efficient reduction in gradients across all the models. The epochs at which a comparatively lower gradient was achieved were also fewer than those needed for the RProp algorithm. Therefore, the LM training algorithm was found to be comparatively more efficient for optimization when compared to the RProp algorithm.

The current study, while providing valuable insights into water quality modeling using artificial neural networks, had some limitations as well. This study employed historical meteorological data and did not incorporate future climate change projections, which could give water quality predictions for long-term hydrological management. Hence, future research could focus on this perspective. Additionally, more training algorithms could be explored and compared. Likewise, the models were trained on the meteorological data of

Bursa and the water quality data of Doğancı dam. However, different environmental and climatic conditions elsewhere may result in slightly different output results. Nevertheless, generally, based on the overall results, it could be concluded that artificial neural networking could be applicable in predicting the water quality of a drinking-water dam. It helped evaluate the effects of the changing climate on water characteristics.

5. Conclusions

In this study, artificial neural networks (ANNs) were effectively applied, mirroring the success seen in prior research. A feed-forward neural network with a distinct layer structure was utilized, and Model 1 emerged as the most effective, demonstrating superior correlation, minimal error, and faster training with a minimum gradient compared to other models. It used key climatic parameters as inputs to predict critical water quality metrics of Doğancı dam. The Levenberg–Marquardt algorithm outperformed the resilient back-propagation algorithm. This research provides valuable insights into the influence of climate indicators on water quality, offering a useful tool for water management and a proactive approach to sustaining drinking-water resources. The developed ANN model could essentially assist engineers and practitioners in government agencies in predicting water quality parameters with the changing weather and atmospheric patterns. This would enable timely interventions, resource planning, and informed decision-making for adaptive strategies to mitigate the impacts of climate change on water resources. This study's methodology could be expanded to explore the effects of climate change on the water levels of drinking-water bodies.

Author Contributions: A.K.: Conceptualization, formal analysis, investigation, methodology, resources, supervision, software, validation, writing—review and editing. A.A.: Formal analysis, investigation, methodology, software, validation, visualization, writing—original draft. All authors have read and agreed to the published version of the manuscript.

Funding: This research received no external funding.

Data Availability Statement: The dataset used in this research for the modeling has been made openly available at Asifa44 (2024). Asifa44/Dataset-for-research: Dataset for water quality of Doğancı dam and meteorology of Bursa (v1.1). Zenodo: https://doi.org/10.5281/zenodo.13837827 (accessed on 31 January 2025, under Creative Commons Attribution 4.0 International Rights).

Acknowledgments: The authors would like to express their gratitude to the Bursa Water and Sewerage Administration (Bursa Su ve Kanalizasyon İdaresi—BUSKİ) and the Meteorological Department of Bursa for their invaluable contribution of datasets, which were essential for the completion of this study. Appreciation is also extended to the State Hydraulic Works (Devlet Su İşleri—DSİ) for their indirect support, which significantly aided this research.

Conflicts of Interest: The authors declare no conflicts of interest.

References

1. Nazari-Sharabian, M.; Taheriyoun, M.; Ahmad, S.; Karakouzian, M.; Ahmadi, A. Water quality modeling of Mahabad Dam watershed–reservoir system under climate change conditions, using SWAT and system dynamics. *Water* **2019**, *11*, 394. [CrossRef]
2. Jeppesen, E.; Brucet, S.; Naselli-Flores, L.; Papastergiadou, E.; Stefanidis, K.; Noges, T.; Noges, P.; Attayde, J.L.; Zohary, T.; Coppens, J. Ecological impacts of global warming and water abstraction on lakes and reservoirs due to changes in water level and related changes in salinity. *Hydrobiologia* **2015**, *750*, 201–227. [CrossRef]
3. Syafii, N.I.; Ichinose, M.; Kumakura, E.; Jusuf, S.K.; Chigusa, K.; Wong, N.H. Thermal environment assessment around bodies of water in urban canyons: A scale model study. *Sustain. Cities Soc.* **2017**, *34*, 79–89. [CrossRef]
4. Hébert, C.; Caissie, D.; Satish, M.G.; El-Jabi, N. Predicting hourly stream temperatures using the equilibrium temperature model. *J. Water Resour. Prot.* **2015**, *7*, 322. [CrossRef]

5. Zhang, Y.; Gao, Q. Comprehensive prediction model of water quality based on grey model and fuzzy neural network. *Chin. J. Environ. Eng.* **2015**, *9*, 537–545.
6. Al-Jarrah, O.Y.; Yoo, P.D.; Muhaidat, S.; Karagiannidis, G.K.; Taha, K. Efficient machine learning for big data: A review. *Big Data Res.* **2015**, *2*, 87–93. [CrossRef]
7. Rajaee, T.; Boroumand, A. Forecasting of chlorophyll-a concentrations in South San Francisco Bay using five different models. *Appl. Ocean Res.* **2015**, *53*, 208–217. [CrossRef]
8. Wang, T.; Chen, W.; Tang, B. Water quality prediction using ARIMA-SSA-LSTM combination model. *Water Supply* **2024**, *24*, 1282–1297. [CrossRef]
9. Nourani, V.; Alami, M.T.; Vousoughi, F.D. Self-organizing map clustering technique for ANN-based spatiotemporal modeling of groundwater quality parameters. *J. Hydroinform.* **2016**, *18*, 288–309. [CrossRef]
10. Garousi-Nejad, I.; Bozorg-Haddad, O.; Loáiciga, H.A.; Mariño, M.A. Application of the firefly algorithm to optimal operation of reservoirs with the purpose of irrigation supply and hydropower production. *J. Irrig. Drain. Eng.* **2016**, *142*, 04016041. [CrossRef]
11. Allawi, M.F.; Jaafar, O.; Mohamad Hamzah, F.; Abdullah, S.M.S.; El-Shafie, A. Review on applications of artificial intelligence methods for dam and reservoir-hydro-environment models. *Environ. Sci. Pollut. Res.* **2018**, *25*, 13446–13469. [CrossRef] [PubMed]
12. Büyükşahin, Ü.Ç.; Ertekin, Ş. Improving forecasting accuracy of time series data using a new ARIMA-ANN hybrid method and empirical mode decomposition. *Neurocomputing* **2019**, *361*, 151–163. [CrossRef]
13. Zare, A.; Bayat, V.; Daneshkare, A. Forecasting nitrate concentration in groundwater using artificial neural network and linear regression models. *Int. Agrophys.* **2011**, *25*, 187–192.
14. Zare Abyaneh, H. Evaluation of multivariate linear regression and artificial neural networks in prediction of water quality parameters. *J. Environ. Health Sci. Eng.* **2014**, *12*, 40. [CrossRef] [PubMed]
15. Vicente, H.; Couto, C.; Machado, J.; Abelha, A.; Neves, J. Prediction of water quality parameters in a reservoir using artificial neural networks. *Int. J. Des. Nat. Ecodyn.* **2012**, *7*, 310–319. [CrossRef]
16. Chen, W.-B.; Liu, W.-C. Artificial neural network modeling of dissolved oxygen in reservoir. *Environ. Monit. Assess.* **2014**, *186*, 1203–1217. [CrossRef]
17. Asadollahfardi, G.; Zangooei, H.; Aria, S.H.; Danesh, E. Application of artificial neural networks to predict total dissolved solids at the Karaj Dam. *Environ. Qual. Manag.* **2017**, *26*, 55–72. [CrossRef]
18. Chou, J.-S.; Ho, C.-C.; Hoang, H.-S. Determining quality of water in reservoir using machine learning. *Ecol. Inform.* **2018**, *44*, 57–75. [CrossRef]
19. Kang, B.; Do Kim, Y.; Lee, J.M.; Kim, S.J. Hydro-environmental runoff projection under GCM scenario downscaled by Artificial Neural Network in the Namgang Dam watershed, Korea. *KSCE J. Civ. Eng.* **2015**, *19*, 434–445. [CrossRef]
20. Zhang, Y.; Huang, J.J.; Chen, L.; Qi, L. Eutrophication forecasting and management by artificial neural network: A case study at Yuqiao Reservoir in North China. *J. Hydroinform.* **2015**, *17*, 679–695. [CrossRef]
21. Saghi, H.; Karimi, L.; Javid, A. Investigation on trophic state index by artificial neural networks (case study: Dez Dam of Iran). *Appl. Water Sci.* **2015**, *5*, 127–136. [CrossRef]
22. Nguyen, H.H.; Recknagel, F.; Meyer, W.; Frizenschaf, J.; Shrestha, M.K. Modelling the impacts of altered management practices, land use and climate changes on the water quality of the Millbrook catchment-reservoir system in South Australia. *J. Environ. Manag.* **2017**, *202*, 1–11. [CrossRef]
23. Wang, J.; Geng, Y.; Zhao, Q.; Zhang, Y.; Miao, Y.; Yuan, X.; Jin, Y.; Zhang, W. Water quality prediction of water sources based on meteorological factors using the CA-NARX Approach. *Environ. Model. Assess.* **2021**, *26*, 529–541. [CrossRef]
24. Özçelik, O. Assessment and Prediction of Water Quality Parameters in Lake Köyceğiz Using Artificial Neural Network Approach. Master's Thesis, Middle East Technical University, Ankara, Turkey, 27 November 2015.
25. Karul, C.; Soyupak, S.; Çilesiz, A.F.; Akbay, N.; Germen, E. Case studies on the use of neural networks in eutrophication modeling. *Ecol. Model.* **2000**, *134*, 145–152. [CrossRef]
26. Sonmez, O.; Dogan, E.; Ceribasi, G.; Demir, S. Impact of climate change on the daily water level fluctuation of Lake Sapanca. *Fresenius Environ. Bull.* **2013**, *22*, 1895–1903.
27. Elhatip, H.; Kömür, M.A. Evaluation of water quality parameters for the Mamasin dam in Aksaray City in the central Anatolian part of Turkey by means of artificial neural networks. *Environ. Geol.* **2008**, *53*, 1157–1164. [CrossRef]
28. Kocsis, T.; Kovács-Székely, I.; Anda, A. Comparison of parametric and non-parametric time-series analysis methods on a long-term meteorological data set. *Cent. Eur. Geol.* **2017**, *60*, 316–332. [CrossRef]
29. Troch, P. *Global Warming and the Acceleration of the Hydrological Cycle*; IAHS Press: Wallingford, UK, 2008.
30. Arkin, P.A.; Smith, T.M.; Sapiano, M.R.; Janowiak, J. The observed sensitivity of the global hydrological cycle to changes in surface temperature. *Environ. Res. Lett.* **2010**, *5*, 035201. [CrossRef]
31. Abbas, M.; Zhao, L.; Wang, Y. Perspective impact on water environment and hydrological regime owing to climate change: A review. *Hydrology* **2022**, *9*, 203. [CrossRef]

32. Pachauri, R.K.; Allen, M.R.; Barros, V.R.; Broome, J.; Cramer, W.; Christ, R.; Church, J.A.; Clarke, L.; Dahe, Q.; Dasgupta, P. *Climate Change 2014: Synthesis Report. Contribution of Working Groups I, II and III to the Fifth Assessment Report of the Intergovernmental Panel on Climate Change*; IPCC: Geneva, Switzerland, 2014; p. 151.
33. Akal Solmaz, S.A.; Yalili, M. Bursanin İçme Suyu Meselesi ve Bazı Çözüm Önerileri. *Ekoloji* **2002**, *11*, 36–39.
34. Ustun, G.E. The Assessment of heavy metal contamination in the waters of the Nilufer Stream in Bursa. *Ekoloji* **2011**, *20*, 61–66. [CrossRef]
35. Vaheddoost, B. Evaluation of Monthly Drought Using Standardized Precipitation Index in Bursa, Turkey. In Proceedings of the 4th Eurasian Conference on Civil and Environmental Engineering, Istanbul, Turkey, 17–18 June 2019; pp. 17–18.
36. Katip, A. Meteorological drought analysis using artificial neural networks for Bursa city, Turkey. *Appl. Ecol. Environ. Res.* **2018**, *16*, 3315–3332. [CrossRef]
37. Kurt, A. Doğancı Baraj Rezervuarı su Kalitesinin Temel Bileşenler Analizi Yardımıyla Değerlendirilmesi. Uludağ Üniversitesi, Türkiye. 2012. Available online: https://www.proquest.com/docview/2606885923?pq-origsite=gscholar&fromopenview=true (accessed on 28 November 2023).
38. Erünal, E. Examining age structure and estimating mortality rates in Ottoman Bursa using mid-nineteenth-century population registers. *Middle East. Stud.* **2020**, *57*, 179–196. [CrossRef]
39. Ozsoy, G.; Aksoy, E.; Karaata, E. Estimating soil loss of Doganci Dam watershed, northwest Turkey and lifetime analyze of Doganci Dam using multi-year remotely sensed data and GIS techniques. *Soil-Water J.* **2013**, *2*, 927–934.
40. Singh, K.P.; Basant, A.; Malik, A.; Jain, G. Artificial neural network modeling of the river water quality—A case study. *Ecol. Model.* **2009**, *220*, 888–895. [CrossRef]
41. Chung, S.W.; Kim, J.H. Development of water quality models for supporting NH3-N control in a dam regulated river. *Water Sci. Technol.* **2005**, *52*, 83–90. [CrossRef] [PubMed]
42. Temizyurek, M.; Dadaser-Celik, F. Modelling the effects of meteorological parameters on water temperature using artificial neural networks. *Water Sci. Technol.* **2018**, *77*, 1724–1733. [CrossRef]
43. Wahir, N.; Nor, M.; Rusiman, M.; Gopal, K. Treatment of outliers via interpolation method with neural network forecast performances. *J. Phys. Conf. Ser.* **2018**, *995*, 012025. [CrossRef]
44. Longyang, Q. Assessing the effects of climate change on water quality of plateau deep-water lake-A study case of Hongfeng Lake. *Sci. Total Environ.* **2019**, *647*, 1518–1530. [CrossRef]
45. USEPA. National Primary Drinking Water Regulations. Available online: https://www.epa.gov/ground-water-and-drinking-water/national-primary-drinking-water-regulations#three:2009 (accessed on 15 July 2023).
46. WHO. Drinking Water Quality Guidelines. 2022. Available online: https://www.who.int/publications/i/item/9789240045064 (accessed on 11 June 2023).
47. Türk Standardlari, E. Türk Standardı TS 266 (Sular-İnsanî Tüketim Amaçlı Sular). 2005. Available online: https://intweb.tse.org.tr/Standard/Standard/Stdard.aspx?081118051115108051104119110104055047105102120088111043113104073100115103084043078075072076065089 (accessed on 20 June 2023).
48. Amer, M.; Maul, T. A review of modularization techniques in artificial neural networks. *Artif. Intell. Rev.* **2019**, *52*, 527–561. [CrossRef]
49. ASCE. Artificial neural networks in hydrology. I: Preliminary concepts. *J. Hydrol. Eng.* **2000**, *5*, 115–123. [CrossRef]
50. Wu, J.S.; Han, J.; Annambhotla, S.; Bryant, S. Artificial neural networks for forecasting watershed runoff and stream flows. *J. Hydrol. Eng.* **2005**, *10*, 216–222. [CrossRef]
51. Zou, J.; Han, Y.; So, S.-S. Overview of artificial neural networks. *Artif. Neural Netw.* **2008**, *458*, 14–22. [CrossRef]
52. Jain, A.K.; Mao, J.; Mohiuddin, K.M. Artificial neural networks: A tutorial. *Computer* **1996**, *29*, 31–44. [CrossRef]
53. Kalin, L.; Isik, S. Prediction of water quality parameters using an artificial neural networks model. In Proceedings of the World Environmental and Water Resources Congress 2010: Challenges of Change, Providence, Rhode Island, 16–20 May 2010; pp. 3145–3153.
54. Svozil, D.; Kvasnicka, V.; Pospichal, J. Introduction to multi-layer feed-forward neural networks. *Chemom. Intell. Lab. Syst.* **1997**, *39*, 43–62. [CrossRef]
55. Ojha, V.K.; Abraham, A.; Snášel, V. Metaheuristic design of feedforward neural networks: A review of two decades of research. *Eng. Appl. Artif. Intell.* **2017**, *60*, 97–116. [CrossRef]
56. Allen, D.M. Mean square error of prediction as a criterion for selecting variables. *Technometrics* **1971**, *13*, 469–475. [CrossRef]
57. Kişi, Ö.; Uncuoğlu, E. Comparison of three back-propagation training algorithms for two case studies. *Indian J. Eng. Mater. Sci.* **2005**, *12*, 434–442.
58. Glorot, X.; Bengio, Y. Understanding the difficulty of training deep feedforward neural networks. In Proceedings of the Thirteenth International Conference on Artificial Intelligence and Statistics, Sardinia, Italy, 13–15 May 2010; pp. 249–256.
59. Buhari, M.; Adamu, S.S. Short-term load forecasting using artificial neural network. In Proceedings of the International Multi-Conference of Engineers and Computer Scientists, Hong Kong, China, 20–22 October 2021; pp. 1–71.

60. Ghumman, A.; Ghazaw, Y.M.; Sohail, A.; Watanabe, K. Runoff forecasting by artificial neural network and conventional model. *Alex. Eng. J.* **2011**, *50*, 345–350. [CrossRef]
61. Barewar, S.D.; Tawri, S.; Chougule, S.S. Experimental investigation of thermal conductivity and its ANN modeling for glycol-based Ag/ZnO hybrid nanofluids with low concentration. *J. Therm. Anal. Calorim.* **2020**, *139*, 1779–1790. [CrossRef]
62. Noor, A.Z.M.; Fauadi, M.; Jafar, F.A.; Bakar, M.H.A. Optimal number of hidden neuron identification for sustainable manufacturing application. *Int. J. Recent Technol. Eng* **2019**, *8*, 2447–2453. [CrossRef]
63. Kheradpisheh, Z.; Talebi, A.; Rafati, L.; Ghaneian, M.T.; Ehrampoush, M.H. Groundwater quality assessment using artificial neural network: A case study of Bahabad plain, Yazd, Iran. *Desert* **2015**, *20*, 65–71.
64. Pontius, F.W.; Brown, K.G.; Chen, C.J. Health implications of arsenic in drinking water. *J. Am. Water Work. Assoc.* **1994**, *86*, 52–63. [CrossRef]
65. Palani, S.; Liong, S.-Y.; Tkalich, P. An ANN application for water quality forecasting. *Mar. Pollut. Bull.* **2008**, *56*, 1586–1597. [CrossRef]
66. Salari, M.; Shahid, E.S.; Afzali, S.H.; Ehteshami, M.; Conti, G.O.; Derakhshan, Z.; Sheibani, S.N. Quality assessment and artificial neural networks modeling for characterization of chemical and physical parameters of potable water. *Food Chem. Toxicol.* **2018**, *118*, 212–219. [CrossRef] [PubMed]
67. Pal, J.; Chakrabarty, D. Effects of input/output parameters on artificial neural network model efficiency for breakthrough contaminant prediction. *Water Supply* **2021**, *21*, 3614–3628. [CrossRef]
68. Soro, L.B.; Gutierrez, J.B.; Ibarra, J.B.G. Solar-Powered Prototype for Investigation and Analysis of Environmental and Meteorological Parameters that May Affect Dissolved Oxygen. In Proceedings of the 2024 IEEE Third International Conference on Power Electronics, Intelligent Control and Energy Systems (ICPEICES), Delhi, India, 26–28 April 2024; pp. 1178–1183.
69. Ebhota, V.C.; Srivastava, V.M. Effect of Architectural Composition of MLP ANN in Neural Network Learning for Signal Power Loss Prediction. *J. Commun.* **2021**, *16*, 20. [CrossRef]
70. Beale, M.H.; Hagan, M.T.; Demuth, H.B. Neural network toolbox. *User's Guide MathWorks* **2010**, *2*, 77–81.
71. Adeloye, A.; De Munari, A. Artificial neural network based generalized storage–yield–reliability models using the Levenberg–Marquardt algorithm. *J. Hydrol.* **2006**, *326*, 215–230. [CrossRef]
72. Park, Y.; Cho, K.H.; Park, J.; Cha, S.M.; Kim, J.H. Development of early-warning protocol for predicting chlorophyll-a concentration using machine learning models in freshwater and estuarine reservoirs, Korea. *Sci. Total Environ.* **2015**, *502*, 31–41. [CrossRef]
73. Goss-Sampson, M. *Statistical Analysis in JASP: A Guide for Students*; JASP: Visakhapatnam, Andhra Pradesh, India, 2019.